www.MaterialsViews.com



# Directional Clustering of Slanted Nanopillars by Elastocapillarity

*Sang Moon Kim, Junsoo Kim, Seong Min Kang, Segeun Jang, Daeshik Kang, Seung Eon Moon, Hong Nam Kim,* and Hyunsik Yoon**

High aspect ratio (HAR) nanostructures have been in great demand since the long and slender geometry provides promising surface characteristics such as high adhesion force and high sensitivity.[1–4] For example, the efforts to mimic the nanohairy structures of gecko foot hairs and the fabrication of nanowire-based sensors well prove the importance of such high aspect ratio nanostructures.[3–6] However, the fabrication process itself requires to be carried out in wet conditions and even the readily fabricated devices can be exposed to wet environments depending on the applications.[1,7,8] And then, the lateral collapse of nanopillars happens during the drying process since the meniscus between the geometry makes them contact each other as the liquid dries. As a result, the nanopillars are clustered with a few tens of them in a cluster after drying the liquid film. This phenomenon is known as "elastocapillarity," since it occurs due to two factors; the elastic deformation of nanopillars and the capillary force among them.[1,9–11]

For years, the clustering of high aspect ratio nanopillars by capillary force has been conceived as an undesirable but inevitable phenomenon. A few researchers have proposed several methods of manipulating the modulus of nanopillars or selectively reinforcing their stem regions via metal deposition to avoid their clustering.[12,13] On the other hand, there have been attempts to numerically analyze the clustering events or to control the number of clustered pillars to build complex structures such as hierarchical and helical assembly by controlling the geometrical factors.[1,11,14] Especially, the clustering nanopillars and nanofilaments have received much attention recently because of their valuable applications such as microelectromechanical system devices, microsensors, plasmonic sensors, bioprobes, and energy devices.[15–19]

According to the previous studies, the clustered nanopillars displayed many complex structures such as top-gathered, winded, and folded forms.[1,20–24] The shape of clustering could be manipulated by controlling the surface chemistry, pillar designs, condensation, directed immersion, and evaporation.[9,10,21] A few studies have demonstrated directional clustering such as the directional bending of folded nanofilaments reported by carbon nanotube forests,[24,25] and most of them have focused on the physics and phenomena of the symmetric clustering. Therefore, experimental and theoretical studies on asymmetric clustering are substantially needed to address the requirements for the directional self-assembly of nanoscale structures by using physically asymmetric interfaces.

Here, we present a strategy to induce the directional clustering of nanopillars by controlling their tilted angles. We prepare regularly spaced nanopillar arrays with different tilted angles of 0°, 15°, 30°, and 45°, and demonstrate their clustering by dispersing and drying a deionized water droplet on them. By observing their clustering patterns, we develop a simple model to explain the features of tilted-angle-dependent clustering, and propose a criterion to classify the continuity of clustering.

The fabrication method of tilted HAR nanopillars was described in detail in the Experimental Section (see Figure S1, Supporting Information). In brief, we fabricated the mold with tilted nanoholes through inclined dry etching and used it to mold the tilted nanopillars with the UV-curable

Prof. S. M. Kim
Department of Mechanical Engineering
Incheon National University
Incheon 406-772, South Korea
Prof. S. M. Kim, Dr. S. M. Kang, S. Jang, Prof. D. Kang
Global Frontier Center for Multiscale Energy System
Seoul National University
Seoul 151-744, South Korea
J. Kim, Dr. S. E. Moon
3D New Devices Research Section
Electronics and Telecommunications Research Institute
Daejeon 305-700, South Korea
Dr. S. M. Kang, S. Jang
Department of Mechanical and Aerospace Engineering
Seoul National University
Seoul 151-742, South Korea
Prof. D. Kang
Department of Mechanical Engineering
Ajou University
Suwon 443-749, South Korea
Dr. H. N. Kim
Center for BioMicrosystems
Brain Science Institute
Korea Institute of Science and Technology
Seoul 136-791, South Korea
E-mail: hongnam.kim@kist.re.kr
Prof. H. Yoon
Department of Chemical and Biomolecular Engineering
Seoul National University of Science & Technology
Seoul 139-743, South Korea
E-mail: hsyoon@seoultech.ac.kr

DOI: 10.1002/smll.201600730

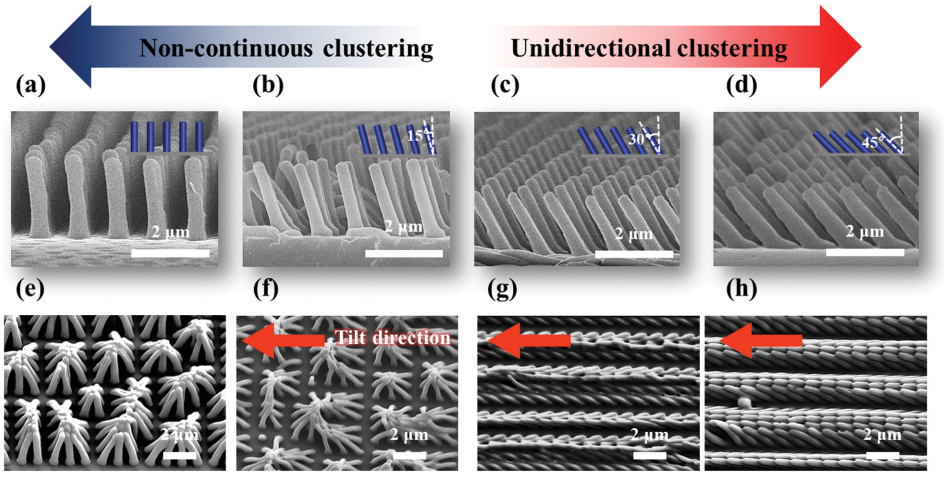


**Figure 1.** Anisotropic clustering of tilted nanopillars via elastocapillarity. Depending on the tilted angles, e,f) noncontinuous or g,h) continuous and unidirectional clustering occurred. a–d) Scanning electron microscopic (SEM) images of the fabricated polymeric nanopillars with the variation of tilting angle a) 0°, b) 15°, c) 30°, and d) 45°, respectively. e–h) SEM images of the clustered nanopillars after the dispensing and drying off water for the patterns with the tilting angle e) ≈0°, f) 15°, g) 30°, and h) 45°, respectively.

polyurethance acrylate polymer (PUA 301). These molded polymeric nanopillar arrays had different tilted angles of 0°, 15°, 30°, and 45° depending on their fabricated molds (**Figure 1**a–d).[4,6] As shown in scanning electron microscopic images, the fabricated HAR nanopillars were arranged in a rectangular shape with high structural fidelity. Furthermore, all these replicated nanopillars had the identical dimensions of ≈480 nm in diameter ($d$), ≈1 μm in pitch ($p$), and ≈1.8 μm in height ($h$) except for their tilted angle.

By using these four different types of regularly spaced tilted HAR nanopillar structures, we observed a clustering phenomenon induced by capillary force in each sample after the deionized water droplet was dried off. Interestingly, the characteristic shapes of the clustering of these four samples were varied according to the different tilting angles of the nanopillars (Figure 1e–h). It is important to note that the clustering condition could be classified into two cases; (i) the noncontinuous and (ii) the continuous and unidirectional clustering. The HAR nanopillars with tilting angles of 0° and 15° were clustered in a discrete island, while those with tilting angles of 30° and 45° showed continuous and unidirectional clustering along their slanted direction. To distinguish between the two apparently different clustering phenomena, the cases of 0° and 15° tiled nanopillars are termed "less-tilted" and 30° and 45°, "more-tilted."

To investigate the unidirectional but noncontinuous clustering, we set first a simple model with straight nanopillars as shown in **Figure 2**a and extend this model to the tilted pillar cases in the later section by including the initial tilting angle $\beta$. The determination of adhesion among the pillars or recovery into original geometry could be calculated by the relative magnitude of their forces.

The clustering induced by capillary force of evaporated liquid (i.e., deionized water) occurs when the capillary force between the pillars exceeds the restoring force of the bent ones. The capillary force ($F_{cap}$) among the pillars can be expressed as their geometrical factors and surface tension of liquid[8,12]

$$F_{cap} = \frac{\pi\gamma d^2\cos^2\theta}{2\sqrt{(d+\rho)^2 - d^2}} \quad (1)$$

where $d$ is the diameter of pillars (480 nm), $\theta$ is the contact angle between liquid and the pillar surface, $\rho$ is the distance among the pillars after bending by the capillary force ($\rho \neq 0$), and $\gamma$ is the surface tension of liquid (water = 72.8 mJ m$^{-2}$). The restoring force of the bent pillars could be expressed as the following equation[4,26,27]

$$F_{res} = \frac{3EI\delta}{h^3} \quad (2)$$

where $E$ is the elastic modulus of the polymer (19.8 MPa),[4] $I$ is the moment of inertia of the pillars $\left(=\frac{\pi r^4}{4}\right)$, $\delta$ is the deflection of pillars from the original location, and $h$ is the height of pillars (1.8 μm).

Then, we calculated the theoretically maximum deflection ($\delta_{max}$) of the nanopillars. For this calculation, we used the assumptions that $\theta$ (contact angle between the water and the pillar surface) is 60° and the distance $\rho$ between the pillars after deflection is 2 nm. The calculated $\delta_{max}$ was 5.7 μm, which is higher than the height of the nanopillars. This implies that capillary force induced clustering happens unavoidably with these geometrical features unless the elastic modulus of polymer changes. Furthermore, we calculated and plotted the capillary force and restoring force with variation of deflection as shown in Figure S2 (Supporting Information). The graph shows that the capillary force is higher than the restoring force even with the variation of deflection, which indicates that the pillars are in the unstable state.

Next, we considered the status of the clustered pillars after drying off the liquid to investigate the maximum number of clustered pillars within a cluster island. In the case, the adhesion force between adjacent pillars induced by van der Waals force and restoring force of bent pillars would

www.MaterialsViews.com

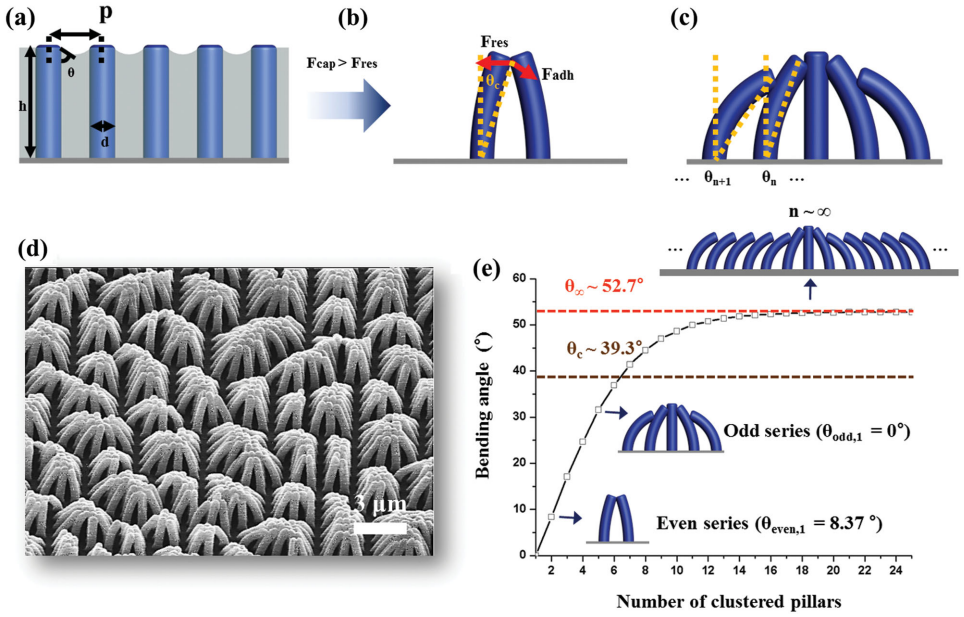


**Figure 2.** Theoretical estimation of the maximum bending angle of nanopillars depending on the number of nanopillars in a cluster island: vertical nanopillar case. a) A model for the capillary force induced clustering. b) A schematic illustration of the cluster formation after drying off the liquid. Two forces, the adhesion force between adjacent pillars and restoring force of bent pillars, compete with each other to determine the cluster formation. c) SEM image of the cluster formation of straight nanopillars. d) A graph for the bending angle with the variation of the number of clustered pillars.

compete with each other as shown in Figure 2b. Here, the restoring force required to bend a nanopillar along the lateral direction is same with the recovery force. A pillar would recover its original shape, if the recovery force exceeds the adhesion force, but if it does not, the pillar would maintain its intimate contact with its adjacent pillars. By assuming that the recovery force is equal to the adhesion force, we can set the critical contact angle ($\theta_c$) and calculate its value through the combination of the aforementioned equations for restoring force and the following equation for adhesion force[4,26]

$$F_{adh} = \frac{Ar^{1/2}l}{16D^{2.5}} \tag{3}$$

where $A$ is the Hamaker constant ($2.09 \times 10^{-20}$ J), $r$ is the radius of pillar (240 nm), $l$ is the overlap length (180 nm; 10% of the pillar height from the observation of the scanning electron microscopic (SEM) images in this paper), and $D$ is the cutoff length between the clustered pillars (0.4 nm). The calculated critical contact angle ($\theta_c$) was ≈39.3°, which means that the nanopillars can adhere to each other only when they are bent less than the $\theta_c$. If the bending angle of a nanopillar is larger than 39.3°, the nanopillar will be detached from the adjacent nanopillars and ultimately restore its vertical shape since the recovery force is larger than the adhesion force.

Based on the results, we calculate the maximum number of clustered pillars. For this calculation, we calculated the tilting angle of every clustered pillar using the geometrically derived recurrence formula as follows (Figure 2c; see the Supporting Information for detailed derivation)

$$\frac{p}{h} = \frac{1}{2\theta_{n+1}} - \frac{1}{2\theta_n} - \frac{1}{2\theta_{n+1}}\cos 2\theta_{n+1} + \frac{1}{2\theta_n}\cos\left(\sin^{-1}\frac{\theta_n}{\theta_{n+1}}\sin 2\theta_{n+1}\right) \tag{4}$$

Although the starting status can be considered as two representative cases depending on whether the first pillar is straight (odd series, $\theta_{odd,1} = 0°$) or bent with its adjacent pillars (even series, $\theta_{even,1} = 8.37°$), both cases appear on one curve, according to the numerical solution, as shown in the graph of Figure 2e, which proves that the initial condition is not critical. The numerical solution of the formula above is limited in one direction (x- or y-orientation only), thus the maximum number of pillars in an island can be found when multiplying the numbers of x- and y-orientations (with the form of $m \times n$). Figure 2d shows the bending angle ($\Delta\theta$) which is the angular deformation from the original state (see the Supporting Information for the derivation). In the case of straight nanopillars which have the initial tilting angle of 0°, they can be clustered up to six in each direction (in x- or y-orientation). When seven pillars are linearly clustered, the last adhered pillar will recover its original shape, which is confirmed by the observation of the SEM image in Figure 2d. Furthermore, we can notice that the bending angle converges to the specific angle (≈52.7°) as the number of clustered pillars increases (Figure 2e). We defined this specific angle as infinite contact angle ($\theta_\infty$), the angle of the infinitely clustering pillars. Therefore, in the case of vertical nanopillars, the bending angle of $n$th nanopillar cannot exceed the infinite contact angle ($\theta_\infty = 52.7°$) theoretically. Notably, this infinite contact angle ($\theta_\infty$) refers to the changed angle from the original state and does not include the initial tilting angle ($\beta$)

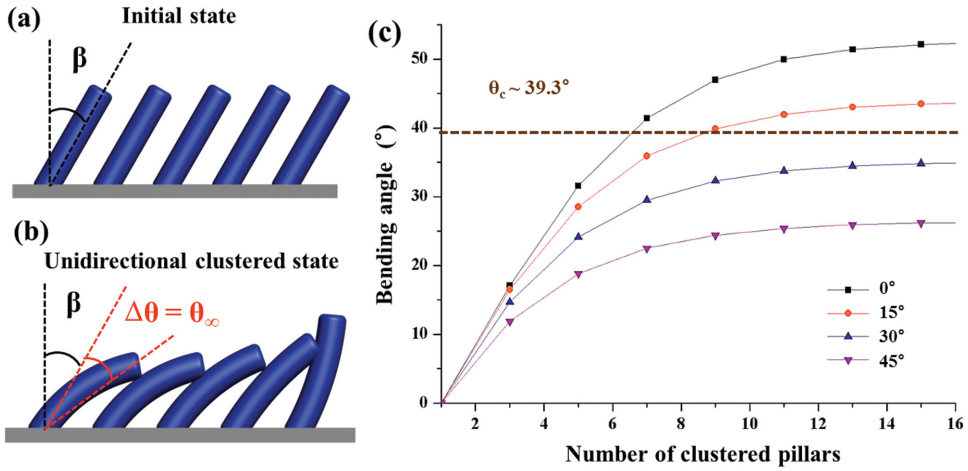


**Figure 3.** Theoretical estimation of the maximum bending angle of nanopillars depending on the number of nanopillars in a cluster island: tilted nanopillar case. a,b) Schematic illustrations for the initial state of the slanted pillars a) and unidirectionally clustered state of the slanted pillars after drying off the liquid b). c) A graph for the bending angle as the number of clustered pillars increase with the variation of initial tilting angle ($\beta$).

($\theta_{total} = \beta + \theta_\infty$). In the case of vertical nanopillars ($\beta = 0°$), the infinite contact angle ($\theta_\infty$) was calculated as ≈52.7°, which is higher than critical contact angle ($\theta_c$) of the pillars (≈39.3°). This implies that the vertical nanopillars will not be clustered with infinite number since the pillars with a bending angle larger than 39.3° will recover their original shape, showing the impossibility of reaching the infinite contact angle ($\theta_\infty$) of 52.7°.

From the result, we gained a clue to set up a criterion for unidirectional clustering, which term refers to how the clustered pillars adhere in one direction continuously and infinitely. Hence, only when the infinite contact angle of pillars is smaller than their critical contact angle ($\theta_c > \theta_\infty$), the bending angle of *n*th pillar can be saturated before the critical contact angle. Finally, infinitely clustered pillars maintain their adhered state. To expand this approach of the criterion for unidirectional clustering to tilted nanopillars, we mathematically calculated the infinite contact angle of the pillars with the variation of the initial tilting angle ($\beta$) used in our experiments ($\beta$ = 15°, 30°, and 45°) (**Figure 3**a,b). The graph in Figure 3c shows that the bending angle of nanopillars was significantly affected by their initial geometrical angle, showing the different saturation angles. Furthermore, the saturation angle can be simply expressed with nondimensional parameter to describe the pillar geometries more generally (Figures S3 and S4; see the Supporting Information for the derivation)

$$\frac{p^*}{h} = -\frac{1}{\theta_\infty}\cos(2\theta_\infty + \beta) \quad (5)$$

where $p^*$ is an effective pitch ($p^* = p - 2R$). The results show that the infinite contact angle of pillars was larger than their critical contact ($\theta_c < \theta_\infty$) in the case of $\beta$ of 0° and 15°, which means that the pillars in this geometrical feature cannot be infinitely clustered. However, in the case of $\beta$ = 30° and 45°, the infinite contact angle of pillars is smaller than their critical contact angle ($\theta_c > \theta_\infty$), which means that they can be clustered infinitely and unidirectionally. The detailed criteria are summarized in **Table 1**.

These theoretical estimations were in good agreement with our experimental results as shown in Figure 1 and Figure S5 (Supporting Information). In addition, to find the exact value of the initial tilting angle, which separates the (i) noncontinuous and (ii) continuous and unidirectional clustering, we plotted the infinite contact angle and the critical contact angle with the variation of the initial tilting angles as shown in **Figure 4**a. The intersecting point of the infinite contact angle and the critical contact angle was calculated as ≈22.8° (initial critical contact angle; $\beta_c$), which implies that the pillars should have a larger initial tilting angle than ≈22.8° to obtain unidirectional clustering toward its tilting direction. Even if the tilted pillars would not be clustered unidirectionally ($\beta$ < 22.8°), they tend to do so anisotropically more in the tilting direction than in the lateral direction. Based on our proposed model, we can also predict the shape of clustered pillars for the case of the noncontinuous clustering as shown in Figure 4b. If we assume the direction #1 as the same direction of the tilting direction, and the direction #2 as its orthogonal direction, then the cluster directionality can be defined as the number of clustered pillars in the direction #2 divided by the number of the pillars in the direction #1. As the initial tilting angle reaches the critical initial contact angle ($\beta_c \approx 22.8°$), the value of cluster directionality converges to zero and the shape would change to a more rectangular one (|) from the square one (■) in the top view (see the Supporting Information for the derivation). Based on the result of continuous and unidirectional clustering effect, we demonstrated an application of optical films in which transmittance

**Table 1.** Criteria for the clustering of nanopillars regarding the magnitude of critical contact angle ($\theta_c$) and the infinite contact angle ($\theta_\infty$).

| Criteria | Results |
|---|---|
| $\theta_\infty > \Delta\theta > \theta_c$ | Recovery |
| $\theta_\infty > \theta_c > \Delta\theta$ | Noncontinuous clustering |
| $\theta_c > \theta_\infty > \Delta\theta$ | Continuous and unidirectional clustering |

www.MaterialsViews.com

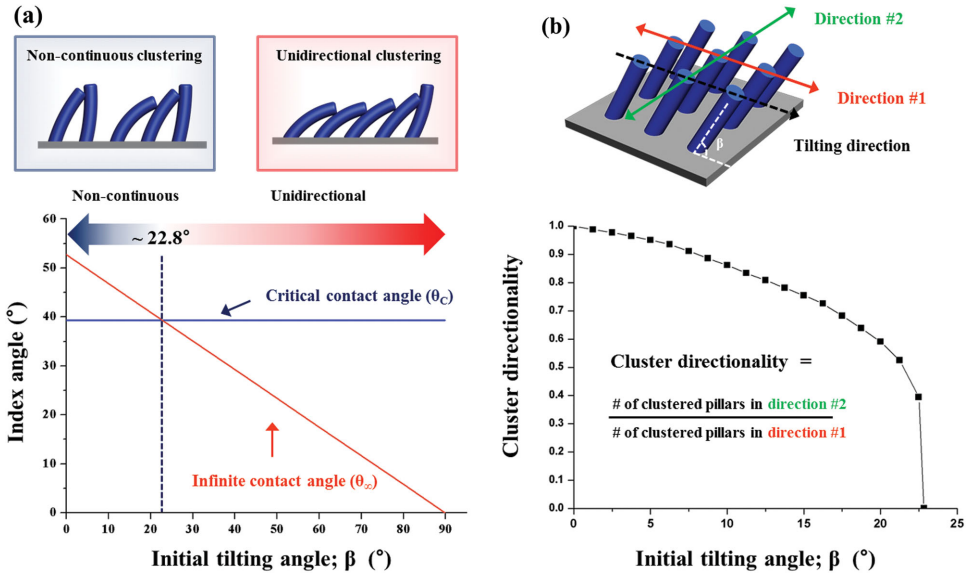


**Figure 4.** The criteria for the regime which classifying noncontinuous and continuous clustering. a) A plot of infinite contact angle ($\theta_\infty$) and critical contact angle ($\theta_c$) with the variation of initial tilting angle to set a criterion for unidirectional clustering. b) A graph for directionality of clustering with the variation of initial tilting angle in the case of noncontinuous clustering.

can be regionally controlled and manipulated as shown in Figure S6 (Supporting Information).

We observed the tilted-angle-dependent clustering of nanopillar arrays after drying the water droplet. It was noncontinuous and island-like with 0° and 15° tilt, but continuous and unidirectional with 30° and 45° tilt. We investigated the phenomenon with a simple model based on the geometrical characteristic of the tilted nanopillars. According to the results, the clustering is determined by the critical contact angle ($\theta_c$) and the unidirectionality (i.e., infinite clustering) by the infinite contact angle ($\theta_\infty$). It implies that the initial tilting angle of the nanopillars is the key factor for their unidirectional clustering. Furthermore, we investigated the maximum number of clustered pillars and their directionality based on our proposed model, and showed that they are in good agreement with the experimental results. The designed asymmetric, directional clustering of tilted nanopillars would be applicable to the directional self-assembly of high aspect ratio nanostructures and directional transport of specific materials.

## Experimental Section

*Preparation of a Si Wafer*: The 4 in. silicon (Si) wafer (Mico MST Co., Korea) used in this experiment was fabricated as follows: First, a *p*-type (100) bare Si wafer with resistivity of 5–30 Ω was cleaned using the solution of 5:1 $H_2O_2$ and $H_2SO_4$. Then, a 500 nm thick $SiO_2$ layer was deposited by the chemical vapor deposition method using tetraethoxysilane on the Si wafer. Finally, the $SiO_2$ layer was patterned by conventional photolithography using AZ1512 photoresist and dry etching techniques. The patterned $SiO_2$ layer acted as a etch mask for the angled etching process.

*Angled Etching Process*: The cleaned Si wafer was cut into pieces by a dicing saw with the dimension of 15 mm × 30 mm. The prepared piece of Si substrate was attached on the holder by using a silver paste to ensure good thermal and electrical contact properties. Then a Faraday cage was mounted over the holder as shown in Figure S1 (Supporting Information). The Faraday cage allowed the modification of the incident angle of plasma ions toward the substrate surface in the conventional dry etching system. The principle of the Faraday cage is described in detail in other previous studies.[5,28] Subsequently, the $SF_6$ and Ar plasma physically etched the Si substrate with the three-different slope angles (15°, 30°, and 45°) of the holder. For the vertical nanoholes, the $SiO_2$ patterned Si wafer specimen was mounted on the horizontal surface of the holder.

*Fabrication of Polymeric Tilted Nanopillars*: A small amount (≈10 µL) of UV-curable PUA prepolymer was drop-dispensed onto the fabricated Si master and covered with a polyethylene-terephthalate (PET) film (thickness: 50 µm). Then, the drop-dispensed PUA prepolymer was exposed by UV light ($\lambda$ = 250 to ≈400 nm) for a few tens of seconds. After the UV-curing process, the solidified PUA replica backed with the PET film was gently peeled off from the Si master (Figure S1, Supporting Information), and further cured with UV for additional 4 h to completely crosslink the polymer.

*Inducing Clustering of Nanopillars*: A 10 µL deionized water droplet was gently dispensed onto the polymeric nanopillar patterns. The water was dried in a dry oven at 50 °C for more than 3 h.

## *Supporting Information*

*Supporting Information is available from the Wiley Online Library or from the author.*

## *Acknowledgements*

*S.M.K., J.K., and S.M.K. contributed equally to this work. This work was supported by the Global Frontier R&D Program in the Center*

*for Multiscale Energy System (NRF-2011-0031561) and the Basic Science Research Program (2013R1A2A2A04015981) funded by the National Research Foundation under the Ministry of Science, ICT & Future Planning, Korea, the R&D Convergence Program of NST (National Research Council of Science & Technology) of Republic of Korea, and the Development of Advanced 3D Printing Technology for the Realistic Artificial Hand funded by KIST-ETRI projects. This research was also supported by Incheon National University Research Grant in 2016 (20162043) and the KIST Institutional Program (2E26664).*

[1] B. Pokroy, S. H. Kang, L. Mahadevan, J. Aizenberg, *Science* **2009**, *323*, 237.
[2] A. Grinthal, S. Kang, A. Epstein, M. Aizenberg, M. Khan, J. Aizenberg, *Nano Today* **2012**, *7*, 35.
[3] C. Pang, G. Y. Lee, T. I. Kim, S. M. Kim, H. N. Kim, S. H. Ahn, K. Y. Suh, *Nat. Mater.* **2012**, *11*, 795.
[4] C. Pang, T. i. Kim, W. G. Bae, D. Kang, S. M. Kim, K. Y. Suh, *Adv. Mater.* **2012**, *24*, 475.
[5] H. E. Jeong, J.-K. Lee, H. N. Kim, S. H. Moon, K. Y. Suh, *Proc. Natl. Acad. Sci. USA* **2009**, *106*, 5639.
[6] C. Pang, S. M. Kim, Y. Rahmawan, K.-Y. Suh, *ACS Appl. Mater. Interfaces* **2012**, *4*, 4225.
[7] F. Chiodi, B. Roman, J. Bico, *EPL* **2010**, *90*, 44006.
[8] D. Chandra, S. Yang, *Langmuir* **2009**, *25*, 10430.
[9] S. H. Kang, B. Pokroy, L. Mahadevan, J. Aizenberg, *ACS Nano* **2010**, *4*, 6323.
[10] M. Matsunaga, M. Aizenberg, J. Aizenberg, *J. Am. Chem. Soc.* **2011**, *133*, 5545.
[11] J. Paulose, D. R. Nelson, J. Aizenberg, *Soft Matter* **2010**, *6*, 2421.
[12] H. Yoon, M. K. Kwak, S. M. Kim, S. H. Sung, J. Lim, H. S. Suh, K. Y. Suh, K. Char, *Small* **2011**, *7*, 3005.
[13] K. Y. Suh, R. Langer, J. Lahann, *Appl. Phys. Lett.* **2003**, *83*, 4250.
[14] M. De Volder, A. J. Hart, *Angew. Chem. Int. Ed.* **2013**, *52*, 2412.
[15] D. N. Futaba, K. Hata, T. Yamada, T. Hiraoka, Y. Hayamizu, Y. Kakudate, O. Tanaike, H. Hatori, M. Yumura, S. Iijima, *Nat. Mater.* **2006**, *5*, 987.
[16] A. Izadi-Najafabadi, S. Yasuda, K. Kobashi, T. Yamada, D. N. Futaba, H. Hatori, M. Yumura, S. Iijima, K. Hata, *Adv. Mater.* **2010**, *22*, E235.
[17] M. A. Correa-Duarte, N. Wagner, J. Rojas-Chapana, C. Morsczeck, M. Thie, M. Giersig, *Nano Lett.* **2004**, *4*, 2233.
[18] Y. Hayamizu, T. Yamada, K. Mizuno, R. C. Davis, D. N. Futaba, M. Yumura, K. Hata, *Nat. Nanotechnol.* **2008**, *3*, 289.
[19] T. Dvir, B. P. Timko, D. S. Kohane, R. Langer, *Nat. Nanotechnol.* **2011**, *6*, 13.
[20] A. Kim, F. S. Ou, D. A. Ohlberg, M. Hu, R. S. Williams, Z. Li, *J. Am. Chem. Soc.* **2011**, *133*, 8234.
[21] H. Duan, J. K. Yang, K. K. Berggren, *Small* **2011**, *7*, 2661.
[22] H. Duan, K. K. Berggren, *Nano Lett.* **2010**, *10*, 3710.
[23] G. Liu, J. Zhou, Y. Xiong, X. Zhang, Y. Tian, *Nanotechnology* **2011**, *22*, 305305.
[24] S. Tawfick, M. De Volder, A. J. Hart, *Langmuir* **2011**, *27*, 6389.
[25] S. Tawfick, Z. Zhao, M. Maschmann, A. Brieland-Shoultz, M. De Volder, J. W. Baur, W. Lu, A. J. Hart, *Langmuir* **2013**, *29*, 5190.
[26] C. Lee, S. M. Kim, Y. J. Kim, Y. W. Choi, K.-Y. Suh, C. Pang, M. Choi, *ACS Appl. Mater. Interfaces* **2015**, *7*, 2561.
[27] W.-G. Bae, M. K. Kwak, H. E. Jeong, C. Pang, H. Jeong, K.-Y. Suh, *Soft Matter* **2013**, *9*, 1422.
[28] H. E. Jeong, J.-K. Lee, M. K. Kwak, S. H. Moon, K. Y. Suh, *Appl. Phys. Lett.* **2010**, *96*, 043704.

Received: March 3, 2016
Revised: April 7, 2016
Published online: June 7, 2016